https://doi.org/10.5194/egusphere-2022-935
Preprint. Discussion started: 4 October 2022

The acceleration of sea-level rise along the coast of the Netherlands started in the 1960s

Iris Keizer[1], Dewi Le Bars[1], Cees de Valk[1], André Jüling[1], Roderik van de Wal[2,3], and Sybren Drijfhout[1,2]

[1]Royal Netherlands Meteorological Institute (KNMI), De Bilt, The Netherlands
[2]Institute for Marine and Atmospheric Research Utrecht, Utrecht University, Utrecht, The Netherlands
[3]Department of Physical Geography, Utrecht University, Utrecht, The Netherlands

Correspondence: Iris Keizer (iris.keizer@knmi.nl)

Abstract.

While a global acceleration of sea-level rise (SLR) during the 20th century is now established, locally acceleration is more difficult to detect because additional processes play a role which sometimes mask the acceleration. Here we study the rate of SLR along the coast of the Netherlands from six tide gauge records, covering the period 1890-2000. We focus on the influence of the wind field and the nodal tide variations on the local sea-level trend. We use four generalised additive models, including different predictive variables, and a parametric bootstrap method to compute the sea-level trend. From the sea-level trend, we obtain the continuous evolution of the rate of SLR and its uncertainty over the observational period through differentiation. Accounting for the nodal cycle only or both the nodal cycle and the wind influence on sea level reduces the standard error in the estimation of the rate of SLR. Moreover, accounting for both the nodal and wind influence changes the estimated rate of SLR, unmasking an acceleration of SLR that started in the 1960s. Our best-fitting statistical model yields a rate of SLR of about $1.8[1.4-2.3]$ mm/yr in 1900-1919 and $1.5[1.1-1.8]$ mm/yr in 1940-1959 compared to $3.0[2.4-3.5]$ mm/yr over 2000-2019. If, apart from tidal, wind effects and fluctuations, sea level would have increased at a constant rate, then the probability (the p-value) of finding a rate difference between 1940-1959 and 2000-2019 of at least our estimate is smaller than 1Our findings can be interpreted as an unequivocal sign of the acceleration of current SLR along the Dutch coast since the 1960s. This aligns with global SLR observations and expectations based on a physical understanding of SLR related to global warming.

A small but significant part of the long-term sea-level trend is due to wind forcing related to a strengthening and northward shift of the jet stream. Additionally, we detect a multidecadal mode of sea-level variability forced by the wind with an amplitude of around 1 cm. We argue that it is related to multi-decadal sea surface temperature variations in the North Atlantic, similar to the Atlantic Multidecadal Variability.

https://doi.org/10.5194/egusphere-2022-935
Preprint. Discussion started: 4 October 2022

1 Introduction

Understanding the current and past rates of sea level rise (SLR) is essential to make reliable sea-level projections and to adapt accordingly. In the Netherlands, the current rate of SLR is used to estimate the volume of sand that must be supplied to maintain the coastline and avoid a retreat of dunes. It also estimates how much salt and gas mining can be allowed under the Wadden Sea. In addition, local sea-level measurements are important to evaluate sea-level projections (Vries et al., 2014) and could be used as an early warning indicator for adaptation measures to uncertain climate change (Haasnoot et al., 2018).

There is now *high confidence* in an acceleration of global SLR in the 20th century compared to the previous three millennia and in the period 2006-2018 compared to 1971-2018 (Fox-Kemper et al., 2021). More recently, Walker et al. (2022) estimated the time when the rate of global SLR emerged from the background variability of the Common Era (0-2000CE) to the middle of the 19th century. For the North-East Atlantic, they found this emergence to occur around the middle of the 20th century. This is in line with Dangendorf et al. (2019) who found a global acceleration of SLR from the 1960s.

Along the coast of the Netherlands, there has been an ongoing debate about whether an acceleration of SLR takes place or not (Baart et al., 2011; Wahl et al., 2013; Steffelbauer et al., 2022). There are multiple lines of evidence that an acceleration should already be detectable or will be detectable soon. Global acceleration of SLR is driven by the increasing thermal expansion of oceans and faster melting glaciers and ice sheets. These mechanisms are also expected to contribute to SLR in the North Sea. However, the contribution of mass loss from the Greenland Ice Sheet is much smaller than the globally averaged contribution due to gravitational effects (Slangen et al., 2012). Additionally, the ocean dynamic sea level is expected to rise along the North-East Atlantic (Lyu et al., 2020; Hermans et al., 2022) and dynamic sea-level projections based on climate models from the Coupled Model Intercomparison Project (CMIP5 and CMIP6) also expect an acceleration. Combined, the expectation for the climate-driven sea-level change along the Dutch coast is close to the global mean changes. (Vries et al., 2014; Fox-Kemper et al., 2021).

The data availability along the Dutch coast is much better than for reconstructed global sea level (Dangendorf et al., 2019; Frederikse et al., 2020). There are six tide gauges measuring sea level with very little missing data since at least 1890. Therefore, it is interesting to study the local acceleration in SLR. The issue with detecting regional acceleration of SLR comes from the large interannual to multidecadal variability from atmospheric forcing, especially important for shallow seas like the North Sea (Gill, 1982; Hermans et al., 2020), and from similar variations in local steric sea level (Bingham and Hughes, 2012). Understanding and removing the interannual to multidecadal sources of variability from tide gauge records was found to be essential for detecting an acceleration of SLR (Haigh et al., 2014). To this end, multilinear regression models between sea levels and atmospheric variables like sea-level pressure gradients, zonal and meridional wind velocity and sometimes precipitation as predictive variables have been used by various authors. For example, this approach was applied to Cuxhaven in the German Bight by Dangendorf et al. (2013) and multiple regions by Calafat and Chambers (2013). Nevertheless, there is no generally agreed approach for detecting an acceleration of SLR from tide gauge stations. Sometimes the observed records are extended by sea-level projections, and the acceleration is defined as a rate of SLR significantly larger than observed, which only allows for finding an acceleration in the future (Haigh et al., 2014; Dangendorf et al., 2014a). Some studies compared the rate between

https://doi.org/10.5194/egusphere-2022-935
Preprint. Discussion started: 4 October 2022

two periods (Calafat and Chambers, 2013; Steffelbauer et al., 2022) and others fitted a second-degree polynomial to the data (Haigh et al., 2014; Dangendorf et al., 2019). In general, the variability due to atmospheric forcing was first estimated by linearly detrending the time series. After that, the variability is removed from the sea level data before estimating the trend and acceleration. Of these previous studies of SLR in the North Sea, many studies did not find evidence of a significant acceleration of SLR (Calafat and Chambers, 2013; Wahl et al., 2013; Haigh et al., 2014; Ezer et al., 2016) whereas Steffelbauer et al. (2022) did. To detect the acceleration of SLR in the North Sea, Steffelbauer et al. (2022) analysed the 100-year time series (1919-2018) of eight tide gauges and found a common breakpoint in the early 1990s. The calculated rate of mean SLR of the stations increases from 1.7 ± 0.3 mm/yr before the breakpoint to 2.7 ± 0.4 mm/yr after the breakpoint implying an acceleration. Moreover, the prior distribution adopted for the rate of SLR before and after the breakpoint assumes that the latter rate can not be smaller than the former rate, which implies that acceleration is assumed from the beginning.

In this paper, we use a new time series approach which uses a Generalised Additive Model (GAM), which allows us to estimate a nonlinear trend and the optimal multilinear regression model simultaneously. The zonal wind and nodal tide are included in the GAM as predictive variables. To reduce the uncertainty in the estimated rate of SLR, only the most important predictor for the atmospheric forcing, the zonal wind, is used, unlike in many previous studies. Also, other authors did not always include the nodal cycle as a predictive variable. Using the GAM, we avoid making strong assumptions about the shape of the sea-level trend like a linear shape as was assumed by Calafat and Chambers (2013); Steffelbauer et al. (2022). The sea-level trend is obtained as a smooth curve representing the long-term change in the data. This trend is then differentiated to compute the rate of SLR. Also, using the GAM allows us to obtain an evolution of the rate of SLR over the observational period, as has not been obtained previously. We also apply a rigorous parametric bootstrap method to estimate the uncertainty in the rate of SLR, which avoids the assumption that the noise is serially uncorrelated. Furthermore, comparing estimates of the rate of SLR with and without the effects of zonal wind and nodal cycle allows us to study the influence of these processes on SLR along the coast of the Netherlands. We also discuss the physical mechanisms driving the wind-driven sea-level variations in the North Sea.

2 Data

2.1 Tide Gauge Observations

Annual-mean sea-level measurements are used from the six reference tide gauges along the coast of the Netherlands: Delfzijl, Den Helder, Harlingen, IJmuiden, Hoek van Holland and Vlissingen. These stations are used for operational sea level monitoring because of their extended temporal coverage and uniform distribution along the Dutch coast (Baart et al., 2019). The measurements are provided by the Permanent Service for Mean Sea Level (Holgate et al., 2013) and were retrieved on November 1st, 2021 from http://www.psmsl.org/data/obtaining/. While the time series for the different stations start between 1862 and 1872, only 1890 to 2020 are used for the analysis. As was done for other studies, tide gauge data is limited to the period after 1890 to avoid the inclusion of a sea-level jump around 1885 (Frederikse and Gerkema, 2018; Baart et al., 2019). From

https://doi.org/10.5194/egusphere-2022-935
Preprint. Discussion started: 4 October 2022

that year, the monthly mean sea level is based on mean sea-level readings rather than mean tide level readings, which could result in a jump in the monthly data (Woodworth, 2017).

2.2 Atmospheric Reanalysis

We use the monthly mean zonal wind at 10 m and atmospheric pressure at sea level from two atmospheric reanalysis products. The first product, the ERA5 reanalysis, from the Copernicus Climate Change service Climate Data Store, is available from 1979 to 2020 with a backward extension to 1950 (Hersbach et al., 2020; Bell et al., 2021). ERA5 has a spatial resolution of $0.25° \times 0.25°$. The second product, the Twentieth Century Reanalysis Version 3 (20CRv3) from the National Oceanographic and Atmospheric Administration (NOAA), is available from 1836 to 2015 (Slivinski et al., 2019). The data from this analysis has a spatial resolution of $1.0° \times 1.0°$.

3 Method

3.1 Statistical Models

Four statistical models were developed and used to unravel the influence of different factors on SLR and to extract the background sea-level trend. All models are based on the Generalised Additive Model (GAM, Hastie and Tibshirani (2017); Wood (2020)) and are estimated by penalised maximum likelihood. Compared to a multi-linear regression model, a GAM replaces the strict assumption of a linear or quadratic shape of the sea-level trend by a sum of many smooth functions. This offers the advantage that we are not required to make a priori assumptions about the shape of the sea-level trend. In our four models, the GAM represents the annual-mean sea level averaged over the six tide gauges as a smooth curve (a linear combination of many smooth cubic B-spline basis functions) plus terms representing the influence of the predictive variables. The smooth curve represents the background variation in sea level to be estimated; its exact meaning depends on the choice of the predictive variables. Its smoothness is controlled by a penalty term subtracted from the log-likelihood, which is proportional to the time-integral of the squared curvature of the smooth term Wood (2020). The penalty term was assigned a weight tuned to match the variance of the smooth curve to the variance of a 30-year average.

The first model estimates the sea-level trend only (*Tr*) without using any predictive variables. This setup is equivalent to assuming we do not know anything about the drivers of SLR. We use this model as a reference to evaluate the improvements achieved by increasing the model complexity. In the second model, the influence of the lunar nodal tide on sea level is added (*TrNc*). Two sinusoidal waves in opposition of phase with unknown amplitude and a fixed period of 18.613 years, the period of the nodal tide potential, are included as a predictive variable for the nodal cycle in the GAM. There has been some debate in the literature about the best way to estimate the influence of the nodal cycle on sea level in the North Sea. Using linear regression to estimate the effect of the nodal tide along the Dutch coast shows an increased magnitude and shift in the phase compared to the equilibrium tides (Baart et al., 2011). However, using a closed sea-level budget, Frederikse et al. (2016) suggested that there is no indication that the nodal cycle deviates from the equilibrium tide in the North Sea between 1958 and 2014. We find that

https://doi.org/10.5194/egusphere-2022-935
Preprint. Discussion started: 4 October 2022

assuming equilibrium tides leaves a large amount of energy in the spectrum close to the period of the nodal cycle. Therefore, we decide to use a linear regression model with an undetermined phase and amplitude but a fixed period as in Baart et al. (2011) even though it might remove some additional variability around the period of nodal tides. Using this second model, the influence of the nodal cycle on the trend and variability of sea level can be studied.

The third and fourth models combine trend, nodal cycle and wind. For the third model, wind effects are included by adding $u|u|$ (*TrNcZw*), where u is the zonal wind from reanalysis averaged over the closest grid cell of each tide gauge (Fig. 1a). This is inspired by the wind stress formulation (Dangendorf et al., 2019) but simplified to keep only the zonal wind component. Along the Dutch coast, the zonal wind is much more important for sea-level changes than the meridional wind (see Figs. 7 and 8 from Frederikse and Gerkema (2018) and Fig. 4 from Dangendorf et al. (2014a)) and both wind components are highly correlated. The fourth model uses a large-scale pressure gradient as a predictive variable for the wind effect on sea level (*TrNcPd*). As in Dangendorf et al. (2014b), we compute the Pearson correlation coefficient between linearly detrended sea level along the Dutch coast and atmospheric pressure at sea level (Fig. 1b). This shows a similar pattern as was previously obtained for the German bight (Dangendorf et al., 2014b). The pattern is characterised by a region of negative correlation over Scandinavia and a positive correlation over southern Europe/northern Africa. Each of these regions defines a box where the average pressure is computed. Then, instead of using the pressure in both boxes as predictive variables as in Dangendorf et al. (2014b), we take the difference between the southern and northern boxes. This adds only one variable to the model and is physically motivated by the fact that the meridional pressure gradient is related to the zonal wind by geostrophy. To cover the period from 1836 to 2020, we combine the variables representing wind effects from the two reanalysis datasets using a linear bias correction method (Casanueva et al., 2013). The ERA5 dataset is used as reference data. The mean and standard deviation of the 20CRv3 pressure and zonal wind time series are adjusted over the overlap period, 1950-2015, to match those of ERA5.

3.2 Analysis of Model Output

The wind influence on sea level can be obtained from the results of the *TrNcZw* and *TrNcPd* GAMs. Once the linear regression coefficients are obtained between 1890 and 2020, the wind influence on sea level can be extended back to 1836, the beginning of the 20CRv3 atmospheric reanalysis. We estimate the wind-driven sea-level trend using a 3rd-degree polynomial fit to the annual-mean data. Also, a spectral analysis is performed on the detrended annual-mean data. The spectra are obtained using a multitaper method (Lees and Park, 1995). To obtain the low-frequency wind influence on sea level, the detrended annual-mean sea level data is smoothed using a local polynomial regression (LOWESS, Cleveland and Devlin (1988)) with a window of 21 years that effectively removes high-frequency variability.

Using our four statistical models, we obtain the background sea-level trend. As a next step, the rate of SLR is obtained from differentiating these estimated smooth sea-level trends. The rates of SLR resulting from the different models do not include the same physical processes. *TrNcZw* and *TrNcPd* do not include the contribution from wind and nodal effects and *TrNc* does not include nodal effects while *Tr* includes all processes.

https://doi.org/10.5194/egusphere-2022-935
Preprint. Discussion started: 4 October 2022

3.3 Uncertainty Computation

To estimate our models from the data, we use a generic method for likelihood-based estimation of GAM (Wood, 2020). It treats the unknown noise terms as independent identically distributed normal random variables. However, checks of the residuals reveal that they are serially correlated, so the independence assumption is not warranted. This does not invalidate the method: since only marginal parameters are estimated, the estimator is consistent under weak assumptions on the dependence; see Section 2 of Cox and Reid (2004). However, serial dependence of the noise affects the covariance of the estimated model parameters, so for deriving confidence intervals and for testing hypotheses, we must account for it. Our estimator for the rate of SLR (the finite difference of the smooth spline estimate of the variation in sea level) is particularly sensitive to low-frequency components of the noise. Our error analysis must account for these subtle aspects of serial dependence. Therefore, we apply a parametric bootstrap method based on the noise spectrum, similar to the Wild Bootstrap version of the technique in Kirch and Politis (2011): we estimate the noise spectrum, using the same method as described in the previous section, and generate random instances of the gaussian process having this spectrum. From these, we obtain instances of the sea level time series by adding the estimates of the non-random terms. Then we apply the GAM-based estimator for our models to each of these instances to obtain an estimate of the rate of SLR. This sample of estimates is used to derive the error statistics and to test hypotheses.

However, because the estimate of the rate of SLR is sensitive to low-frequency noise, we cannot assume that the noise spectrum is sufficiently closely approximated by the spectrum of the residuals, as Kirch and Politis (2011) do. Therefore, we need to estimate the noise spectrum from the spectrum of the residuals. A simple iterative correction scheme solves this inverse problem. Given a guess of the noise spectrum, we simulate random instances of sea level time series as above. For each, we estimate the model coefficients, derive the residuals, estimate their spectrum and average these estimates. The quotient of this average to the guess is the mean effect of model estimation. The spectrum of the residuals is then corrected by dividing it by this quotient. The result is used as a guess for the next step. The iteration is initialised with the spectrum of the residuals. It converges within 3 to 5 iterations. The spectrum of the residuals and the estimated noise spectrum differ only in the low frequencies, as some of the noise in this band is absorbed in the spline term.

4 Results

4.1 Comparison of the Different GAMs

The GAM progressively better fits the data, measured by the deviance (Tbl. 1), as the complexity of the model increases (e.g., the number of predictive variables increases), measured by the number of degrees of freedom (Tbl. 1). The deviance is used to compare generalised linear models and is a generalisation of the sum of squares of residuals used to compare linear regression models (Wood, 2020). Including the nodal cycle reduces the deviance by 12%, and including the wind further reduces the deviance by an additional 37% for *TrNcPd* to 58% for *TrNcZw* implying that the best fit is obtained for *TrNcZw*. The improved

https://doi.org/10.5194/egusphere-2022-935
Preprint. Discussion started: 4 October 2022

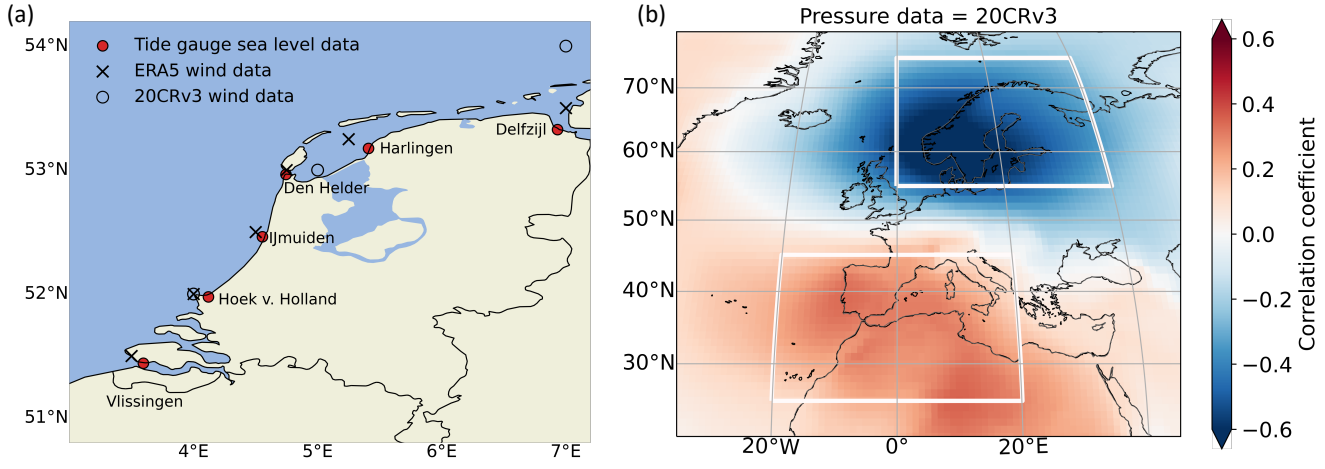

Figure 1. (a) Location of the six tide gauges used to define the mean sea level along the Dutch coast and of the zonal wind data used from the atmospheric reanalyses. (b) The correlation coefficient between sea level along the Dutch coast and atmospheric pressure at sea level from 20CRv3 reanalysis between 1890 and 2015. Both variables are linearly detrended.

Statistical model	Degrees of freedom	Deviance
Tr : Trend only	4.6	1167
TrNc : Trend and nodal tide	6.6	1031
TrNcPd : Trend, nodal tide and wind (pressure)	7.6	652
TrNcZw : Trend, nodal tide and wind (velocity)	7.6	428

Table 1. Summary of statistical model performance. The number of degrees of freedom includes the number of predictive variables and the number of basis functions used by the B-spline method. The deviance is a generalisation of the sum of squares of residuals used to compare linear regression models.

fit for *TrNcZw* could be explained by the fact that here the local zonal wind is used, whereas for *TrNcPd*, a simplification of large-scale zonal wind is used.

The resulting fits can be seen in Fig. 2. When more predictive variables for the wind are included in the model, like the meridional wind or wind taken at multiple locations in the North Sea, the deviance can be further reduced. However, the
185 increased degrees of freedom increase the standard error in estimating the trend (not shown). Therefore, we find that using only one predictive variable for the wind is the best choice for estimating the sea-level trend.

https://doi.org/10.5194/egusphere-2022-935
Preprint. Discussion started: 4 October 2022

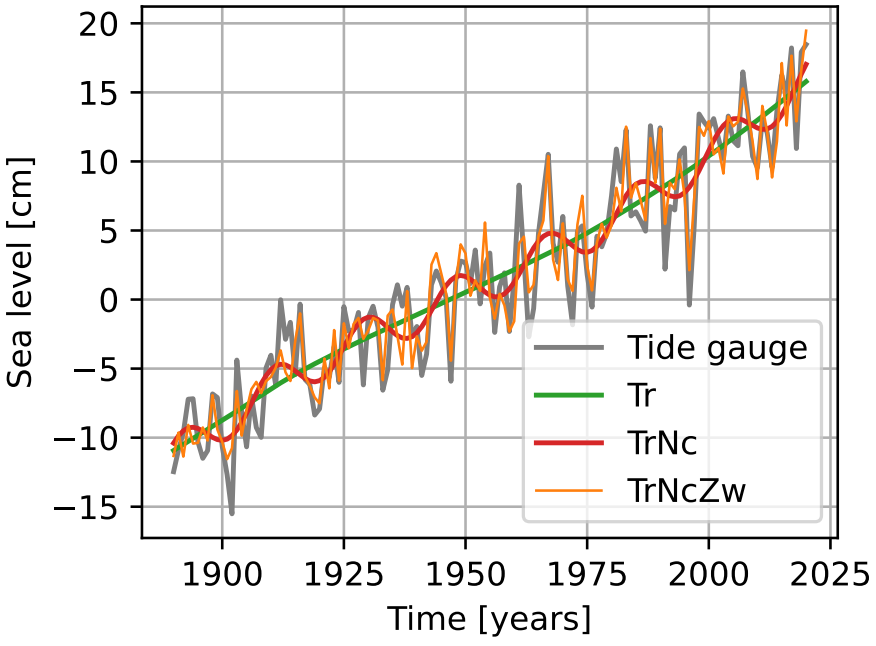

Figure 2. Comparison of the annual tide gauge data averaged over 6 tide gauges along the Dutch coast with three Generalised Additive Models (*Tr*, *TrNc*, *TrNcZw*)

4.2 Wind Influence on Sea Level

Figure 3a shows the resulting wind influence on sea level, where the large interannual variability stands out. From these annual-mean time series, we estimate the wind-driven sea-level trend as is shown in Fig. 3b. For the second period, 1928-2020, the wind-driven trend is 0.12 mm/yr and 0.15 mm/yr for respectively *TrNcZw* and *TrNcPd*. Long-term strengthening of the zonal wind has increased the sea level along the coast of the Netherlands. This long-term strengthening of the zonal wind is consistent with the observed northward shift and increased speed of the jet stream, which could be due to a decreasing temperature gradient between the North Pole and the equator at the height of the tropopause (Fig. 7d and 9d from Hallam et al. (2022)). A long-term influence of atmospheric drivers (zonal and meridional wind and surface pressure) was found earlier for the period 1953-2003 (Fig. 2c from Dangendorf et al. (2014a)), but our results are in contradiction with the atmospheric-driven sea-level drop over the period 1900-2011 found by the same authors. This could be due to an update in the atmospheric reanalysis (20CRv3 instead of 20CRv2).

After removing the trend from the data in Fig. 3a, a spectral analysis is performed (Fig. 3c). The spectra of the wind-impact on sea level obtained using both *TrNcZw* and *TrNcPd* have a similar shape, but the total variance is larger for *TrNcZw* compared to *TrNcPd* which is a result of the larger interannual variability of *TrNcZw* as shown in Fig. 3a. For both methods, there is more

https://doi.org/10.5194/egusphere-2022-935
Preprint. Discussion started: 4 October 2022

energy in the signal for periods larger than two decades than for smaller periods. Therefore, the signals are smoothed using a local polynomial regression (LOWESS, Cleveland and Devlin (1988)) with a window of 21 years that effectively removes high-frequency variability (dashed lines in Fig. 3c). The resulting detrended and smoothed time series, Fig. 3d, show that low-frequency wind variability can raise or drop sea level by over 2 cm over a period of 2 to 5 decades. In App. A, this low-frequency variability lags low-frequency sea-surface temperatures in the North Atlantic that have a similar pattern as the Atlantic Multidecadal Variability.

4.3 Rates of SLR

The rates of SLR obtained from differentiating the estimated smooth sea-level trend from each of the four models are shown in Fig. 4. Reduction of uncertainty is generally the main motivation for removing variability due to known atmospheric drivers from the sea-level trend (Dangendorf et al., 2014a). The rate of change from *TrNc* has lower uncertainty than the rate from *Tr*. Including the zonal wind (*TrNcZw*) as a predictive variable further decreases the uncertainty, whereas including the pressure difference (*TrNcPd*) increases the uncertainty again. The standard error in estimating the trend is larger at the time series' start and end because there are fewer constraints than in the middle of the time series.

In addition to reducing the uncertainty, the wind also influences the rate of SLR itself. Both *TrNcZw* and *TrNcPd* have lower rates in the first part of the 20th century compared to *Tr* and *TrNc*. From the 1960s onward, the rates of SLR of *TrNcZw* and *TrNcPd* increase rapidly. The *TrNcZw* model has the smallest standard error and estimates the largest rate of SLR over recent decades, which reached $3.0[2.4-3.5]$ mm/yr over the period 2000-2019. For this model, the rate of SLR over periods before the acceleration in the 1960s is $1.8[1.4-2.3]$ mm/yr over the period 1900-1920, $1.7[1.3-2.0]$ mm/yr over the period 1920-1940 and $1.5[1.1-1.8]$ mm/yr over the period 1940-1960. Table 2 shows for the different GAMs the probability (the p-value) that the estimated rate difference between the periods 2000-2019 and a previous period (1900-1919, 1920-1939 and 1940-1959) would exceed the rate difference found in this study if the sea level had changed at a constant rate. For the *Tr* model, we find probabilities between 5 and 23% for the different periods. Having more predictive variables in the GAM decreases these probabilities. For the *TrNC* model, the probability is 14% when compared with the period 1900-1919 due to the higher rates of SLR of this model at the beginning of the 20th century. However, for the other periods, we find probabilities of 1%, implying that finding these rate differences would be *very unlikely* if there would have been no acceleration (Mastrandrea et al., 2011). For the *TrNcZw* model, we find probabilities of 0% for all periods, and in the *TrNcPd* model, we find probabilities smaller than 5% and only 1% when compared with the period 1940-1959. These probabilities indicate that an acceleration of SLR is *virtually certain* (Mastrandrea et al., 2011). We conclude that along the coast of the Netherlands, the sea level has accelerated since the 1960s, but this acceleration has been masked by wind-field and nodal-tide variations. This agrees with the global mean sea level that has accelerated since the 1960s (Dangendorf et al., 2019).

All models indicate a decrease in the rate of SLR from the beginning of the 20th century until about 1960", with a minimum in the 1940s for *Tr* and *TrNc* and in the 1960s for *TrNcZw* and *TrNcPd*. This decreasing rate of SLR could be due to the strong Arctic warming from 1900 to 1930, followed by an Arctic cooling from 1930 to 1970 (Fig. 4, Bokuchava and Semenov (2021)). This could have influenced sea level through glacier mass loss followed by gain or local steric sea level changes. Since the

https://doi.org/10.5194/egusphere-2022-935
Preprint. Discussion started: 4 October 2022

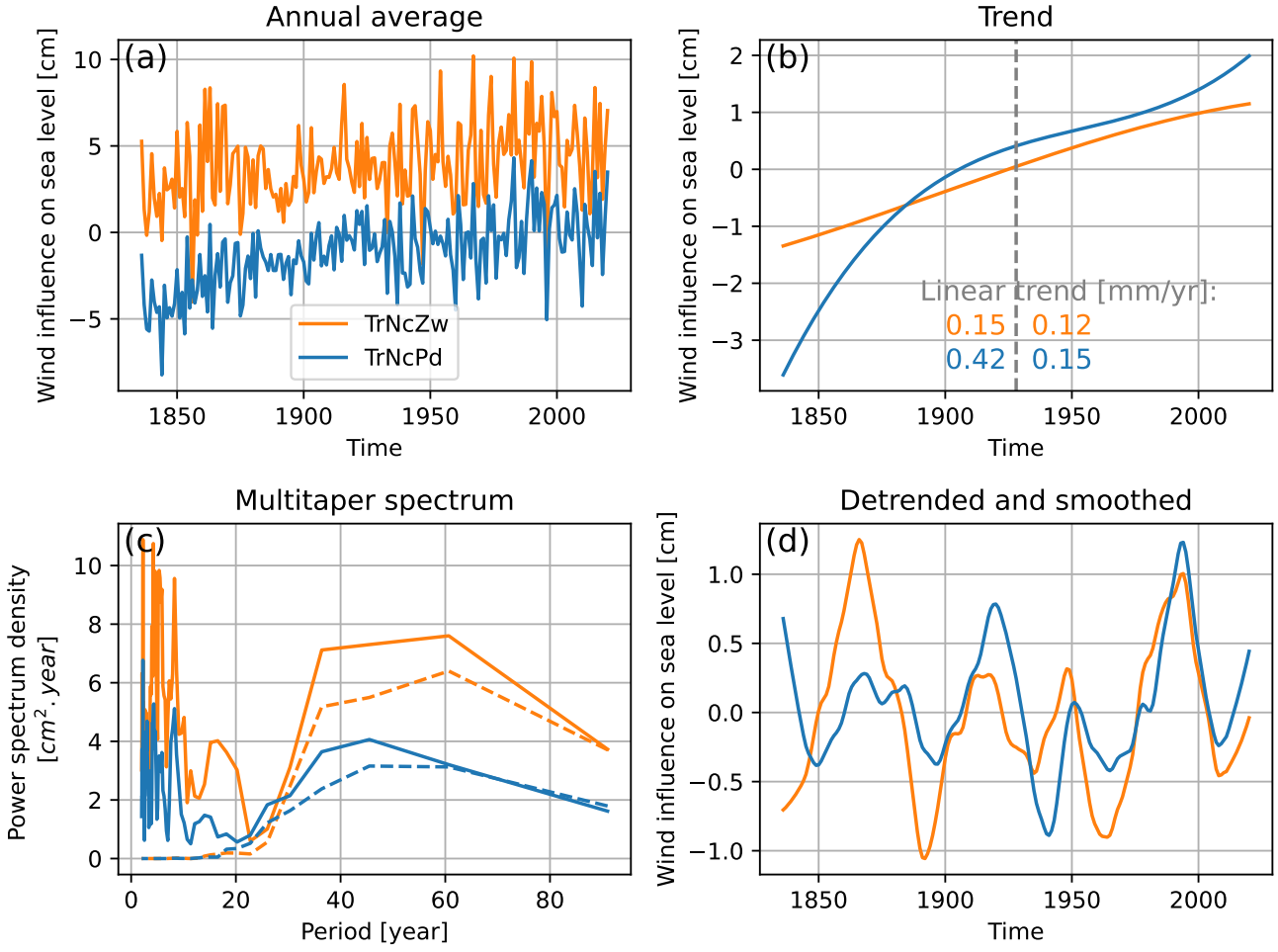

Figure 3. Comparison of the wind influence on sea level along the Dutch coast obtained from two different regressors: average zonal wind of the 6 tide gauge stations (*TrNcZw*) and the pressure difference between the Northern and Southern boxes (*TrNcPd*) of Figure 1. (a) Time series of annual averages. (b) Trend computed using a 3rd-degree polynomial fit with linear trend values over the first half and the second half of the total period. (c) Spectra obtained using a multitaper method (Lees and Park, 1995). Both the detrended time series (solid lines) and the detrended and smoothed time series (dashed lines) are shown. Smoothing is obtained from a LOWESS method with a window of 21 years. (d) Smoothed time series.

https://doi.org/10.5194/egusphere-2022-935
Preprint. Discussion started: 4 October 2022

Statistical model	$r_{2000-2019}$ vs $r_{1900-1919}$	$r_{2000-2019}$ vs $r_{1920-1939}$	$r_{2000-2019}$ vs $r_{1940-1959}$
Tr	0.23	0.06	0.05
TrNc	0.14	0.01	0.01
TrNcZw	< 0.01	< 0.01	< 0.01
TrNcPd	0.05	0.02	0.01

Table 2. P-values represent the probability that the estimated rate difference between 2000-2019 and a previous period before 1960 would exceed the computed value if the actual rates were equal during these two periods. For example, for the *Tr* model, if the sea level rates were the same between 1900-1919 and 2000-2019, then there would be a probability of 0.24 to compute a rate difference at least as large as what we measure. On the other hand, for the model *TrNcZw*, the probability of obtaining a rate difference at least as large as measured under the assumption that the rates are the same is 0.00 for all past periods considered here.

local sea-level budget is not closed before 1950 (Frederikse et al., 2020), we can only speculate about the causes of the drop in the rate of SLR.

5 Discussion

Estimating the trend, nodal cycle and atmospheric processes underlying the wind influence on sea level using the GAM allows for avoiding a priori assumptions about the sea-level trend, like having a linear or quadratic shape, while performing the regression analysis. Thereby, the rate of SLR can be computed as a time-evolving variable over the whole observational period contrary to being calculated as a constant over an arbitrary period as was done in Calafat and Chambers (2013); Steffelbauer et al. (2022). In addition, we propose a careful uncertainty analysis accounting for serially dependent unexplained fluctuations, which is used to evaluate the strength of evidence for an acceleration. These two elements help to avoid framing the problem of acceleration detection as binary. This is important when advising decision-makers: significance testing based on ad hoc models like a broken line trend may lead to a paradigm shift from a steady rate of SLR in one year to an accelerating rise a few years later, as demonstrated by the results in (Calafat and Chambers, 2013; Steffelbauer et al., 2022). To our best knowledge, the GAM has not been applied to estimate trends and acceleration in sea-level data before, and we believe it could help solve similar acceleration detection problems in regions other than the coast of the Netherlands.

When removing the wind influence from the sea-level observations, the underlying assumption is that this influence is only due to natural variability and that there is no structural change due to anthropogenic forcing. However, as we find a wind-driven trend over the entire period of study 1836-2020 from both the zonal wind and pressure difference model, the trend could also continue in the future. We do not know of any study investigating the possible cause of this trend. If it is caused by climate change due to anthropogenic forcing, it would be reasonable to expect it to continue in the future. Otherwise, if it is caused by natural variability, it might reverse. Most of the CMIP5 and CMIP6 ensembles do not show a systematic trend associated with wind influence on sea level in the North Sea, not over the historical period or in future scenarios. So, they either miss the

https://doi.org/10.5194/egusphere-2022-935
Preprint. Discussion started: 4 October 2022

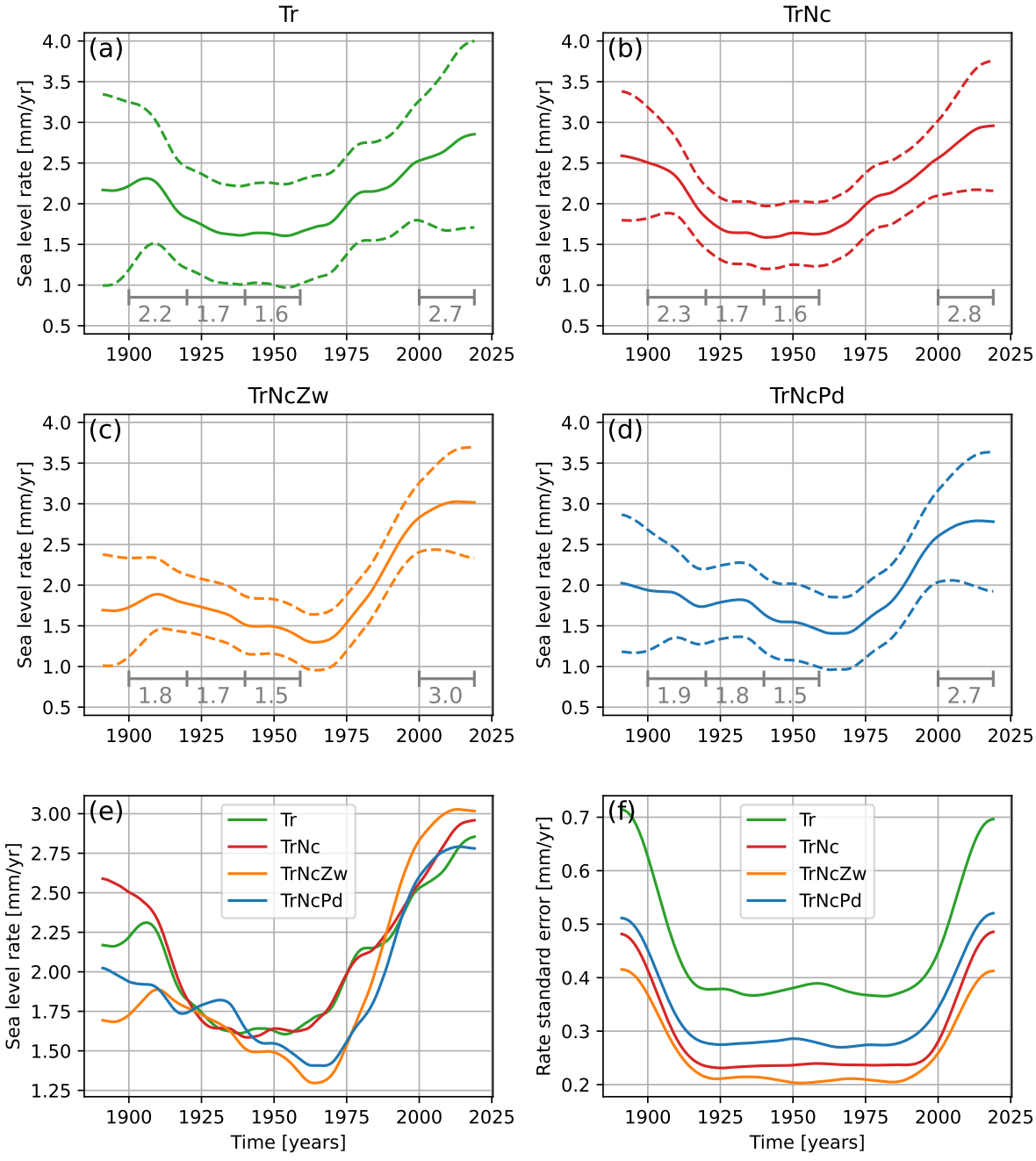

Figure 4. (a–d) The rates of SLR were obtained for four different statistical models. A window of three years is used, so the rates cannot be computed for the first and last years of the time series. The period shown here is 1891 to 2019. The dashed lines show the 5th and 95th percentiles of the uncertainty range computed from a parametric bootstrap method. Numbers in grey under the curves indicate the mean rates for four different periods ([1900-1919], [1920-1939], [1940-1959], [2000-2019]) (e) Median sea level rates. (f) Standard error of the sea level rates.

https://doi.org/10.5194/egusphere-2022-935
Preprint. Discussion started: 4 October 2022

process driving the trend in the observations, or the trend in the comments has to be attributed to natural variability. In each case, the magnitude of around 0.15 mm/yr over the historical period is small enough compared to other sources of uncertainty to neglect it when making sea level projections on time scales of more than several decades.

If the time lag found between North Atlantic SST and wind influence on sea level as described in App. A was found to be physical or if the SST signal could be skillfully forecasted, this relation could provide a source of predictability for the deviation between sea level along the Dutch coast and large-scale drivers (e.g. glacier and ice sheet mass loss, global steric...) at the decadal time scale.

From the daily to the interannual time scale, the wind influence on sea level in shallow seas is well understood by the barotropic theory of the interplay between the Coriolis force, pressure gradient and surface wind stress (equation 3 from Mangini et al. (2021)). On the multidecadal time scale, as investigated in this study, it is possible that the physical mechanism underpinning the relation between wind and sea level also involves steric sea level change (Chen et al., 2014). In particular, baroclinic signals in the deep ocean propagating as a volume flux on shallow seas (Bingham and Hughes, 2012; Calafat et al., 2012). However, since we use the large interannual variability to define the regression coefficient, we think these coefficients mostly reflect the barotropic wind influence.

We find a strong increase in the rate of SLR between the 1960s and 2000s (Fig. 4). From 2000 onward, the standard error of the rate of SLR increases strongly, and it is uncertain whether the increase of the rate persists. A potential application to this increase would be the extrapolation of the observed rate into the near future. This method was recently used as an additional line of evidence for future sea-level rise by Sweet et al. (2022). Based on Fig. 4c, assuming a constant rate of 3 mm/yr from 20000 onwards, we arrive at a rise of 0.3 m between 2000 and 2100, which is slightly higher than the rise over the 20th century. However, assuming a constant acceleration of 1.5/25= 0.06 mm/yr^2 (as inferred from the trend in sea level rate over 1975-2000 in Fig. 4c), we obtain a rise of 0.6 m, from 2000 to 2100, which is twice the rise without acceleration. Given the complexity of changes in the various drivers of global SLR, it would be naive to assume that the acceleration will remain constant during the remainder of this century. However, these crude extrapolations illustrate the practical significance of our estimates of the local rates of SLR and the importance of obtaining the evolution of these rates over time.

6 Conclusions

In this study, we estimate the sea-level trend and the influence of the nodal cycle and wind on sea level along the coast of the Netherlands. We used the average of the observations from six tide gauges and zonal wind and atmospheric pressure at sea level from two reanalysis data sets. Using a set of four GAMs, we estimated the trend using B-splines functions and the wind influence using linear regression. The four models include either no predictive variables, only the nodal cycle, and, additionally, either zonal wind or pressure gradient as predictive variables. We find that using only one predictive variable for the wind best estimates the sea-level trend. The deviance is reduced when more predictive variables are added to the GAM, reducing by 12% for adding the nodal cycle and another 37 to 59% for adding the wind.

https://doi.org/10.5194/egusphere-2022-935
Preprint. Discussion started: 4 October 2022

We obtain the wind influence on sea level using the two GAMs that include a wind predictive variable (*TrNcZw* and *TrNcPd*). Obtaining the wind influence with two different approaches shows the method's robustness as both methods lead to similar conclusions. We find a long-term sea-level rise due to wind forcing of 0.12 mm/yr or 0.15 mm/yr for 1928-2020, depending on the used model. The long-term strengthening of the zonal wind is consistent with an observed northward shift and jet stream strengthening (Hallam et al., 2022). Also, we find a low-frequency wind variability which can rise or drop sea level by about 1 cm over 2 to 5 decades. We find that it is related to multi-decadal sea surface temperature variations in the North Atlantic with a similar pattern as the Atlantic Multidecadal Variability. The correlation between SST in the northern part of the North Atlantic and the multidecadal wind-driven sea-level variability can be understood as smaller SST values increase the meridional temperature gradient and strengthen the jet stream (Hallam et al., 2022). In summary, we find both a long-term SLR as well as a multidecadal sea-level variability due to wind forcing which are both connected to changes in the jet stream through various mechanisms (Hallam et al., 2022).

After obtaining the sea-level trend using the four GAMs, we obtain the rate of SLR by differentiating the trend. This results in new insight into the evolution of the rate of SLR along the coast of the Netherlands over the observational period. The rates of SLR, excluding the influence of the wind, are lower at the beginning of the 20th century and larger at the beginning of the 21st century. Our best-fitting model yields a rate of SLR, excluding nodal and wind effects, of $3.0[2.4-3.5]$ mm/yr over 2000-2019 compared to $1.8[1.4-2.3]$ mm/yr in 1900-1919 and $1.5[1.1-1.8]$ mm/yr in 1940-1959. The probability (the p-value) of finding a rate difference between 1940-1959 and 2000-2019 equal to the one we found when there would not have been an acceleration is smaller than 1%. From these results, we conclude that an acceleration of SLR is *virtually certain*. Also, we find, for the first time, that the acceleration of SLR along the coast of the Netherlands started in the 1960s. This aligns with global SLR observations and expectations based on a physical understanding of SLR related to global warming (Fox-Kemper et al., 2021; Dangendorf et al., 2019). Furthermore, we explain that the acceleration of SLR along the Dutch coast has been difficult to detect due to the masking of the acceleration by wind-field and nodal-tide variations.

Code and data availability. Currently, all data and code can be found in the GitHub repository: https://github.com/KNMI-sealevel/NetherlandsSeaLevelAcceleration. After the review process, when a final version of the code and data is obtained, the code and data will be uploaded to Zotero and a DOI will be provided.

https://doi.org/10.5194/egusphere-2022-935
Preprint. Discussion started: 4 October 2022

Appendix A: Low-frequency wind influence on sea level

After smoothing the wind influence on sea level, we found a low-frequency wind-driven sea-level signal with an amplitude of over 1 cm and a period of 2 to 5 decades (Fig. 3d). Previous authors have not shown this wind-driven low-frequency sea-level variability, and it has therefore not been discussed what processes might drive this sea-level variability. The North Atlantic Oscillation (NAO) has already been shown to influence the sea level in the North Sea, especially in the winter (Jevrejeva et al., 2005; Dangendorf et al., 2012, 2014a). This is not surprising given how close the correlation pattern in Fig. 1b is to the NAO.

To go one step further, we look at the relation between low-frequency wind influence on sea level and low-frequency sea surface temperature (SST) in the North Atlantic using linear regression. We use monthly SST data from two reanalysis products. The COBE-SST2 reanalysis dataset from NOAA has a temporal coverage from 1850 to 2019 (Hirahara et al., 2014). The HadISSTv1.1 reanalysis dataset from the Met Office Hadley Centre has a temporal coverage from 1870 to the present, but the data of the incomplete year, 2022, are excluded from our analysis (Rayner et al., 2003). Both data sets have a resolution of $1.0° \times 1.0°$. We obtain the low-frequency sea surface temperature by detrending and smoothing the time series. Again, the smoothing is obtained using a LOWESS method with a window of 21 years. We perform a linear regression to reconstruct the low-frequency wind influence using the low-frequency sea surface temperature as a predictive variable. By performing the regression for each grid point in the North Atlantic, we obtain a correlation pattern for this region.

This shows that the multidecadal wind-driven sea-level variability can be related to North Atlantic SSTs. Figures A1a and c show the correlation pattern for the North Atlantic for *TrNcZw* and *TrNcPd*. In this figure, we only show the results for COBE-SST2 data since the results obtained using HadISSTv1.1 are similar. In a few regions, the SST is strongly correlated, especially in the tropics, north of the equator (box "South") and around Iceland in the Irminger Sea and southern Norwegian Sea (box "North"), where the SST explains more than 50% of the variance of wind influence on sea level (not shown). For these boxes and a large region of the North Atlantic, generally used to define the Atlantic Multidecadal Variability (AMV, Jüling et al. (2020)), we obtain the area-averaged low-frequency SST. Again, we obtain the relation to low-frequency wind influence on sea level using linear regression, including the SST data as a lagged dependent variable for lags from -40 to 40 years (Fig. A1b, d). The wind influence is negatively correlated with past SST for positive time lags. A few years after the SST reaches a minimum in one of these regions, the wind pushes the sea level to a maximum along the Dutch coast. We find that, depending on the case, the correlation coefficient is between -0.3 and -0.7 at lag 0. However, the negative correlation becomes stronger with a positive time lag and reaches a minimum for a lag between 3 and 10 years. Here, SST can explain between 35 and 65% of the variance in wind-driven sea-level variability. We also see that the time lag is smaller for the North and South region than for the AMV region. While SST can explain an important part of multidecadal variability for both *TrNcZw* and *TrNcPd*, the correlation is stronger for *TrNcPd*.

The relation between SST in the "North" box and zonal wind can be understood physically. A minimum temperature in this region would tend to increase the meridional temperature gradient and strengthen the jet stream (Hallam et al., 2022). Understanding the physical relationship between SST in the other boxes and the sea level in the North Sea, given the potential time lag, is not straightforward. Given the noise in the signal, the smoothing could be responsible for this lag, so it is not certain

https://doi.org/10.5194/egusphere-2022-935
Preprint. Discussion started: 4 October 2022

that this is a physical feature. We also noticed that the lag increases for increased smoothing (not shown). The uncertainties of the correlations shown in Fig. A1b and d are represented by the standard error. However, both time series are smoothed, causing their autocorrelation to increase and the sample size n to alter. Therefore, the uncertainties shown in Fig. A1b and d are underestimated.

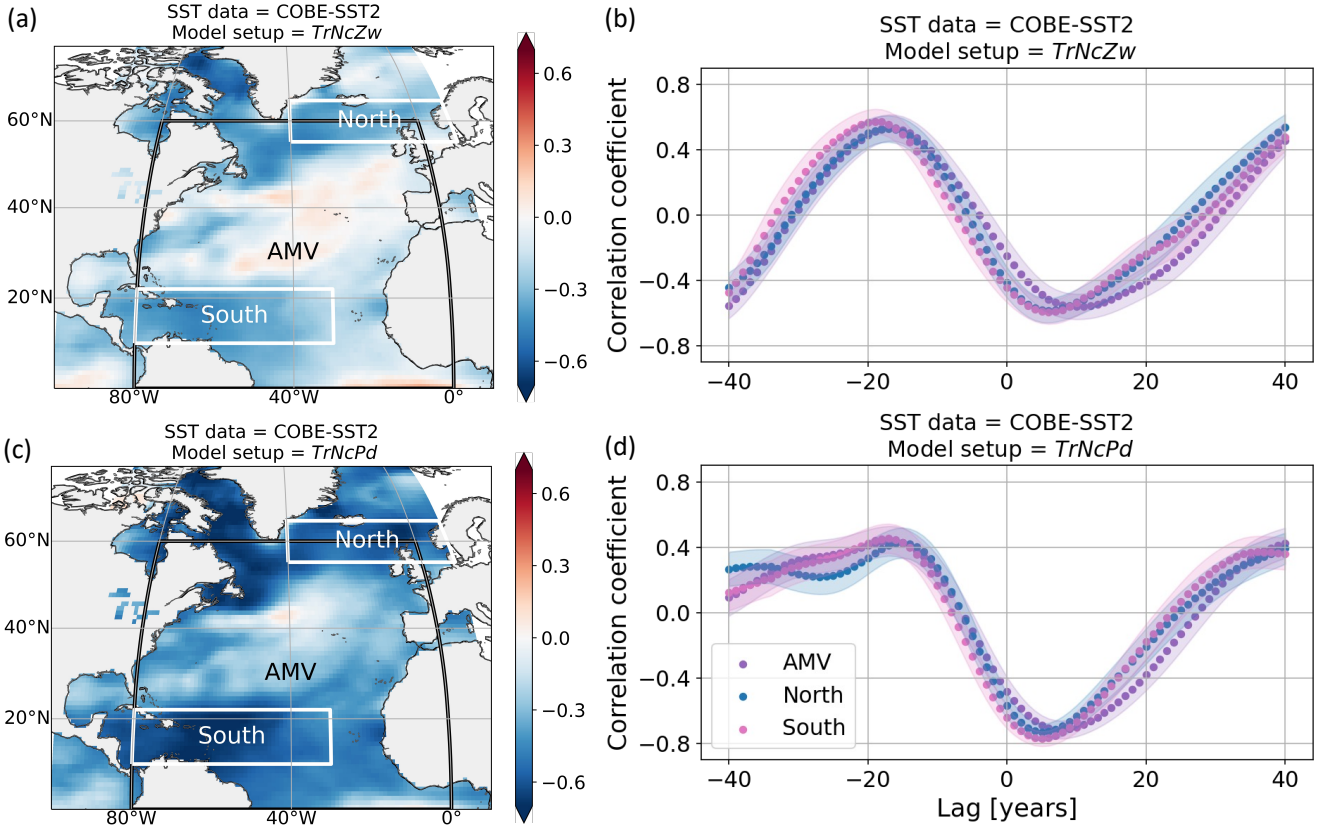

Figure A1. (a) and (c) Maps of the correlation coefficients between the wind influence on sea level along the Dutch coast for *TrNcZw* and *TrNcPd* using COBE-SST2 data. Both variables are detrended and smoothed. (b) and (d) represent the regression coefficients for, respectively, *TrNcZw* and *TrNcPd*, three regions of the North Atlantic and different time lags. Linear regressions are performed over the longest available period: 1850 - 2019. The shaded areas show 1 standard error of the correlation coefficients (r) is shown, $\sigma_r = (1 - r^2)/\sqrt{n-2}$, with n the length of the time series.

Author contributions. Iris Keizer, Dewi Le Bars and Cees de Valk developed the model code and performed the simulations. All authors contributed to the interpretation of results. Iris Keizer and Dewi Le Bars prepared the manuscript with contribution from all authors.

https://doi.org/10.5194/egusphere-2022-935
Preprint. Discussion started: 4 October 2022

Competing interests. The authors declare that they have no conflict of interest.

Acknowledgements. This publication was supported by the project RECEIPT (REmote Climate Effects and their Impact on European sustainability, Policy and Trade) which received funding from the European Union's Horizon 2020 Research and Innovation Programme under Grant agreement No. 820712 and by PROTECT a European Union's Horizon 2020 research and innovation program under grant agreement No. 869304.

Iris Keizer, Dewi Le Bars and Sybren Drijfhout gratefully acknowledge support from the Netherlands Knowledge Programme on Sea-level rise that supported them with a special grant. Roderik van de Wal and André Jüling acknowledge support from the Netherlands Polar Program to the Dutch Polar Climate and Cryosphere Change Consortium.

In this study, we used the GAM implementation, Lowess filtering and third-order detrending tool from the statsmodel library (https://www.statsmodels.org/; Seabold and Perktold (2010)), the multitaper method from the spectrum library (https://pyspectrum.readthedocs.io) and the ordinary least squares regression model from the scikit-learn library (https://scikit-learn.org).

https://doi.org/10.5194/egusphere-2022-935
Preprint. Discussion started: 4 October 2022

References

Baart, F., van Gelder, P. H. A. J. M., de Ronde, J., van Koningsveld, M., and Wouters, B.: The Effect of the 18.6-Year Lunar Nodal Cycle on Regional Sea-Level Rise Estimates, Journal of Coastal Research, 28, 511–516, https://doi.org/10.2112/JCOASTRES-D-11-00169.1, 2011.

Baart, F., Rongen, G., Hijma, M., Kooi, H., de Winter, R., and Nicolai, R.: Zeespiegelmonitor 2018: De stand van zaken rond de zeespiegelstijging langs de Nederlandse kust, Tech. rep., https://deltalife.deltares.nl/deltares/de_nederlandse_delta/zeespiegelstijging/160368/Zeespiegelmonitor_2018_final.pdf, 2019.

Bell, B., Hersbach, H., Simmons, A., Berrisford, P., Dahlgren, P., Horányi, A., Muñoz-Sabater, J., Nicolas, J., Radu, R., Schepers, D., Soci, C., Villaume, S., Bidlot, J.-R., Haimberger, L., Woollen, J., Buontempo, C., and Thépaut, J.-N.: The ERA5 global reanalysis: Preliminary extension to 1950, Quarterly Journal of the Royal Meteorological Society, 147, 4186–4227, https://doi.org/10.1002/qj.4174, _eprint: https://onlinelibrary.wiley.com/doi/pdf/10.1002/qj.4174, 2021.

Bingham, R. J. and Hughes, C. W.: Local diagnostics to estimate density-induced sea level variations over topography and along coastlines: TOPOGRAPHY AND SEA LEVEL, Journal of Geophysical Research: Oceans, 117, https://doi.org/10.1029/2011JC007276, 2012.

Bokuchava, D. D. and Semenov, V. A.: Mechanisms of the Early 20th Century Warming in the Arctic, Earth-Science Reviews, 222, 103 820, https://doi.org/10.1016/j.earscirev.2021.103820, 2021.

Calafat, F. M. and Chambers, D. P.: Quantifying recent acceleration in sea level unrelated to internal climate variability, Geophysical Research Letters, 40, 3661–3666, https://doi.org/10.1002/grl.50731, 2013.

Calafat, F. M., Chambers, D. P., and Tsimplis, M. N.: Mechanisms of decadal sea level variability in the eastern North Atlantic and the Mediterranean Sea, Journal of Geophysical Research: Oceans, 117, https://doi.org/https://doi.org/10.1029/2012JC008285, 2012.

Casanueva, A., Herrera, S., Fernández, J., Frías, M. D., and Gutiérrez, J. M.: Evaluation and projection of daily temperature percentiles from statistical and dynamical downscaling methods, Natural Hazards and Earth System Sciences, 13, 2089–2099, https://doi.org/10.5194/nhess-13-2089-2013, publisher: Copernicus GmbH, 2013.

Chen, X., Dangendorf, S., Narayan, N., O'Driscoll, K., Tsimplis, M. N., Su, J., Mayer, B., and Pohlmann, T.: On sea level change in the North Sea influenced by the North Atlantic Oscillation: Local and remote steric effects, Estuarine, Coastal and Shelf Science, 151, 186–195, https://doi.org/10.1016/j.ecss.2014.10.009, 2014.

Cleveland, W. S. and Devlin, S. J.: Locally Weighted Regression: An Approach to Regression Analysis by Local Fitting, Journal of the American Statistical Association, 83, 596–610, https://doi.org/10.1080/01621459.1988.10478639, publisher: Taylor & Francis _eprint: https://www.tandfonline.com/doi/pdf/10.1080/01621459.1988.10478639, 1988.

Cox, D. R. and Reid, N.: A note on pseudolikelihood constructed from marginal densities, Biometrika, 91, 729–737, https://doi.org/https://doi.org/10.1093/biomet/91.3.729, publisher: Oxford University Press, 2004.

Dangendorf, S., Wahl, T., Hein, H., Jensen, J., Mai, S., and Mudersbach, C.: Mean Sea Level Variability and Influence of the North Atlantic Oscillation on Long-Term Trends in the German Bight, Water, 4, 170–195, https://doi.org/10.3390/w4010170, 2012.

Dangendorf, S., Mudersbach, C., Wahl, T., and Jensen, J.: Characteristics of intra-, inter-annual and decadal sea-level variability and the role of meteorological forcing: the long record of Cuxhaven, Ocean Dynamics, 63, 209–224, https://doi.org/10.1007/s10236-013-0598-0, 2013.

Dangendorf, S., Calafat, F. M., Arns, A., Wahl, T., Haigh, I. D., and Jensen, J.: Mean sea level variability in the North Sea: Processes and implications, Journal of Geophysical Research: Oceans, 119, https://doi.org/10.1002/2014JC009901, 2014a.

https://doi.org/10.5194/egusphere-2022-935
Preprint. Discussion started: 4 October 2022

Dangendorf, S., Wahl, T., Nilson, E., Klein, B., and Jensen, J.: A new atmospheric proxy for sea level variability in the southeastern North Sea: observations and future ensemble projections, Climate Dynamics, 43, 447–467, https://doi.org/10.1007/s00382-013-1932-4, 2014b.

Dangendorf, S., Hay, C., Calafat, F. M., Marcos, M., Piecuch, C. G., Berk, K., and Jensen, J.: Persistent acceleration in global sea-level rise since the 1960s, Nature Climate Change, 9, 705–710, https://doi.org/10.1038/s41558-019-0531-8, 2019.

Ezer, T., Haigh, I. D., and Woodworth, P. L.: Nonlinear Sea-Level Trends and Long-Term Variability on Western European Coasts, Journal of Coastal Research, 32, 744–755, https://doi.org/10.2112/JCOASTRES-D-15-00165.1, publisher: Coastal Education and Research Foundation, 2016.

Fox-Kemper, B., Hewitt, H. T., Xiao, C., Aðalgeirsdóttir, G., Drijfhout, S. S., Edwards, T. L., Golledge, N. R., Hemer, M., Kopp, R. E., Krinner, G., Mix, A., Notz, D., Nowicki, S., Nurhati, I. S., Ruiz, L., Sallée, J. B., and Slangen, A. B. A.: Ocean, Cryosphere and Sea Level Change. In: Climate Change 2021: The Physical Science Basis. Contribution of Working Group I to the Sixth Assessment Report of the Intergovernmental Panel on Climate Change [Masson-Delmotte, V., P. Zhai, A. Pirani, S. L. Connors, C. Péan, S. Berger, N. Caud, Y. Chen, L. Goldfarb, M. I. Gomis, M. Huang, K. Leitzell, E. Lonnoy, J.B.R. Matthews, T. K. Maycock, T. Waterfield, O. Yelekçi, R. Yu and B. Zhou (eds.)], Cambridge University Press, 2021.

Frederikse, T. and Gerkema, T.: Multi-decadal variability in seasonal mean sea level along the North Sea coast, Ocean Science, 14, 1491–1501, https://doi.org/10.5194/os-14-1491-2018, publisher: Copernicus GmbH, 2018.

Frederikse, T., Riva, R., Kleinherenbrink, M., Wada, Y., van den Broeke, M., and Marzeion, B.: Closing the sea level budget on a regional scale: Trends and variability on the Northwestern European continental shelf, Geophysical Research Letters, 43, 10,864–10,872, https://doi.org/10.1002/2016GL070750, 2016.

Frederikse, T., Landerer, F., Caron, L., Adhikari, S., Parkes, D., Humphrey, V. W., Dangendorf, S., Hogarth, P., Zanna, L., Cheng, L., and Wu, Y.-H.: The causes of sea-level rise since 1900, Nature, 584, 393–397, https://doi.org/10.1038/s41586-020-2591-3, number: 7821 Publisher: Nature Publishing Group, 2020.

Gill, A. E.: Atmosphere-Ocean Dynamics, Academic Press, google-Books-ID: 1WLNX_lfRp8C, 1982.

Haasnoot, M., van 't Klooster, S., and van Alphen, J.: Designing a monitoring system to detect signals to adapt to uncertain climate change, Global Environmental Change, 52, 273–285, https://doi.org/10.1016/j.gloenvcha.2018.08.003, 2018.

Haigh, I. D., Wahl, T., Rohling, E. J., Price, R. M., Pattiaratchi, C. B., Calafat, F. M., and Dangendorf, S.: Timescales for detecting a significant acceleration in sea level rise, Nature Communications, 5, 3635, https://doi.org/10.1038/ncomms4635, 2014.

Hallam, S., Josey, S. A., McCarthy, G. D., and Hirschi, J. J.-M.: A regional (land–ocean) comparison of the seasonal to decadal variability of the Northern Hemisphere jet stream 1871–2011, Climate Dynamics, https://doi.org/10.1007/s00382-022-06185-5, 2022.

Hastie, T. J. and Tibshirani, R. J.: Generalized Additive Models, Routledge, New York, https://doi.org/10.1201/9780203753781, 2017.

Hermans, T. H. J., Bars, D. L., Katsman, C. A., Camargo, C. M. L., Gerkema, T., Calafat, F. M., Tinker, J., and Slangen, A. B. A.: Drivers of Interannual Sea Level Variability on the Northwestern European Shelf, Journal of Geophysical Research: Oceans, 125, e2020JC016 325, https://doi.org/https://doi.org/10.1029/2020JC016325, _eprint: https://agupubs.onlinelibrary.wiley.com/doi/pdf/10.1029/2020JC016325, 2020.

Hermans, T. H. J., Katsman, C. A., Camargo, C. M. L., Garner, G. G., Kopp, R. E., and Slangen, A. B. A.: The Effect of Wind Stress on Seasonal Sea-Level Change on the Northwestern European Shelf, Journal of Climate, 35, 1745–1759, https://doi.org/10.1175/JCLI-D-21-0636.1, publisher: American Meteorological Society Section: Journal of Climate, 2022.

Hersbach, H., Bell, B., Berrisford, P., Hirahara, S., Horányi, A., Muñoz-Sabater, J., Nicolas, J., Peubey, C., Radu, R., Schepers, D., Simmons, A., Soci, C., Abdalla, S., Abellan, X., Balsamo, G., Bechtold, P., Biavati, G., Bidlot, J., Bonavita, M., De Chiara, G., Dahlgren,

https://doi.org/10.5194/egusphere-2022-935
Preprint. Discussion started: 4 October 2022

P., Dee, D., Diamantakis, M., Dragani, R., Flemming, J., Forbes, R., Fuentes, M., Geer, A., Haimberger, L., Healy, S., Hogan, R. J., Hólm, E., Janisková, M., Keeley, S., Laloyaux, P., Lopez, P., Lupu, C., Radnoti, G., de Rosnay, P., Rozum, I., Vamborg, F., Villaume, S., and Thépaut, J.-N.: The ERA5 global reanalysis, Quarterly Journal of the Royal Meteorological Society, 146, 1999–2049, https://doi.org/10.1002/qj.3803, _eprint: https://onlinelibrary.wiley.com/doi/pdf/10.1002/qj.3803, 2020.

Hirahara, S., Ishii, M., and Fukuda, Y.: Centennial-Scale Sea Surface Temperature Analysis and Its Uncertainty, Journal of Climate, 27, 57–75, https://doi.org/10.1175/JCLI-D-12-00837.1, publisher: American Meteorological Society Section: Journal of Climate, 2014.

Holgate, S. J., Matthews, A., Woodworth, P. L., Rickards, L. J., Tamisiea, M. E., Bradshaw, E., Foden, P. R., Gordon, K. M., Jevrejeva, S., and Pugh, J.: New Data Systems and Products at the Permanent Service for Mean Sea Level, Journal of Coastal Research, 29, 493–504, https://doi.org/10.2112/JCOASTRES-D-12-00175.1, publisher: Coastal Education and Research Foundation, 2013.

Jevrejeva, S., Moore, J., Woodworth, P., and Grinsted, A.: Influence of large-scale atmospheric circulation on European sea level: results based on the wavelet transform method, Tellus A: Dynamic Meteorology and Oceanography, 57, 183–193, https://doi.org/10.3402/tellusa.v57i2.14609, publisher: Taylor & Francis _eprint: https://doi.org/10.3402/tellusa.v57i2.14609, 2005.

Jüling, A., Dijkstra, H. A., Hogg, A. M., and Moon, W.: Multidecadal variability in the climate system: phenomena and mechanisms, The European Physical Journal Plus, 135, 506, https://doi.org/10.1140/epjp/s13360-020-00515-4, 2020.

Kirch, C. and Politis, D. N.: TFT-bootstrap: Resampling time series in the frequency domain to obtain replicates in the time domain, The Annals of Statistics, 39, 1427–1470, https://doi.org/10.1214/10-AOS868, publisher: Institute of Mathematical Statistics, 2011.

Lees, J. M. and Park, J.: Multiple-taper spectral analysis: A stand-alone C-subroutine, Computers & Geosciences, 21, 199–236, https://doi.org/10.1016/0098-3004(94)00067-5, 1995.

Lyu, K., Zhang, X., and Church, J. A.: Regional Dynamic Sea Level Simulated in the CMIP5 and CMIP6 Models: Mean Biases, Future Projections, and Their Linkages, Journal of Climate, 33, 6377–6398, https://doi.org/10.1175/JCLI-D-19-1029.1, publisher: American Meteorological Society, 2020.

Mangini, F., Chafik, L., Madonna, E., Li, C., Bertino, L., and Nilsen, J. E. : The relationship between the eddy-driven jet stream and northern European sea level variability, Tellus A: Dynamic Meteorology and Oceanography, 73, 1–15, https://doi.org/10.1080/16000870.2021.1886419, publisher: Taylor & Francis _eprint: https://doi.org/10.1080/16000870.2021.1886419, 2021.

Mastrandrea, M. D., Mach, K. J., Plattner, G.-K., Edenhofer, O., Stocker, T. F., Field, C. B., Ebi, K. L., and Matschoss, P. R.: The IPCC AR5 guidance note on consistent treatment of uncertainties: a common approach across the working groups, Climatic Change, 108, 675, https://doi.org/10.1007/s10584-011-0178-6, 2011.

Rayner, N. A., Parker, D. E., Horton, E. B., Folland, C. K., Alexander, L. V., Rowell, D. P., Kent, E. C., and Kaplan, A.: Global analyses of sea surface temperature, sea ice, and night marine air temperature since the late nineteenth century, Journal of Geophysical Research: Atmospheres, 108, https://doi.org/10.1029/2002JD002670, _eprint: https://onlinelibrary.wiley.com/doi/pdf/10.1029/2002JD002670, 2003.

Seabold, S. and Perktold, J.: statsmodels: Econometric and statistical modeling with python, in: 9th Python in Science Conference, 2010.

Slangen, A. B. A., Katsman, C. A., van de Wal, R. S. W., Vermeersen, L. L. A., and Riva, R. E. M.: Towards regional projections of twenty-first century sea-level change based on IPCC SRES scenarios, Climate Dynamics, 38, 1191–1209, https://doi.org/10.1007/s00382-011-1057-6, 2012.

Slivinski, L. C., Compo, G. P., Whitaker, J. S., Sardeshmukh, P. D., Giese, B. S., McColl, C., Allan, R., Yin, X., Vose, R., Titchner, H., Kennedy, J., Spencer, L. J., Ashcroft, L., Brönnimann, S., Brunet, M., Camuffo, D., Cornes, R., Cram, T. A., Crouthamel, R., Domínguez-Castro, F., Freeman, J. E., Gergis, J., Hawkins, E., Jones, P. D., Jourdain, S., Kaplan, A., Kubota, H., Blancq, F. L., Lee, T.-C., Lorrey, A.,

https://doi.org/10.5194/egusphere-2022-935
Preprint. Discussion started: 4 October 2022

Luterbacher, J., Maugeri, M., Mock, C. J., Moore, G. K., Przybylak, R., Pudmenzky, C., Reason, C., Slonosky, V. C., Smith, C. A., Tinz, B., Trewin, B., Valente, M. A., Wang, X. L., Wilkinson, C., Wood, K., and Wyszyński, P.: Towards a more reliable historical reanalysis: Improvements for version 3 of the Twentieth Century Reanalysis system, Quarterly Journal of the Royal Meteorological Society, 145, 2876–2908, https://doi.org/10.1002/qj.3598, _eprint: https://onlinelibrary.wiley.com/doi/pdf/10.1002/qj.3598, 2019.

Steffelbauer, D. B., Riva, R. E. M., Timmermans, J. S., Kwakkel, J. H., and Bakker, M.: Evidence of regional sea-level rise acceleration for the North Sea, Environmental Research Letters, 17, 074 002, https://doi.org/10.1088/1748-9326/ac753a, publisher: IOP Publishing, 2022.

Sweet, W., Hamlington, B., Kopp, R., and Weaver, C.: Global and Regional Sea Level Rise Scenarios for the United States: Up- dated Mean Projections and Extreme Water Level Probabilities Along U.S. Coastlines., NOAA Technical Report NOS 01, National Oceanic and Atmospheric Administration, National Ocean Service, Silver Spring, MD, 111 pp, https://oceanservice.noaa.gov/hazards/sealevelrise/noaa-nos-techrpt01-global-regional-SLR-scenarios-US.pdf, 2022.

Vries, H. d., Katsman, C., and Drijfhout, S.: Constructing scenarios of regional sea level change using global temperature pathways, Environmental Research Letters, 9, 115 007, https://doi.org/10.1088/1748-9326/9/11/115007, 2014.

Wahl, T., Haigh, I., Woodworth, P., Albrecht, F., Dillingh, D., Jensen, J., Nicholls, R., Weisse, R., and Wöppelmann, G.: Observed mean sea level changes around the North Sea coastline from 1800 to present, Earth-Science Reviews, 124, 51–67, https://doi.org/10.1016/j.earscirev.2013.05.003, 2013.

Walker, J. S., Kopp, R. E., Little, C. M., and Horton, B. P.: Timing of emergence of modern rates of sea-level rise by 1863, Nature Communications, 13, 966, https://doi.org/10.1038/s41467-022-28564-6, number: 1 Publisher: Nature Publishing Group, 2022.

Wood, S. N.: Inference and computation with generalized additive models and their extensions, TEST, 29, 307–339, https://doi.org/10.1007/s11749-020-00711-5, 2020.

Woodworth, P. L.: Differences between mean tide level and mean sea level, Journal of Geodesy, 91, 69–90, https://doi.org/10.1007/s00190-016-0938-1, 2017.